Patterns of Coherent Decadal and Interdecadal Climate Signals in the Pacific Basin during the 20th Century

Yves M. Tourre[1], Balaji Rajagopalan[1], Yochanan Kushnir[1], Mathew Barlow[2]
Warren B. White[3]

Abstract. Two distinct low-frequency fluctuations are suggested from a joint frequency domain analysis of the Pacific Ocean (30°S-60°N) sea surface temperature (SST) and sea level pressure (SLP). The lowest frequency signal reveals a spatially coherent interdecadal evolution. In-phase SST and SLP anomalies are found along the subarctic frontal zone (SAFZ). It is symmetric about the equator, with tropical SST anomalies peaking near 15° latitudes in the eastern Pacific. The other low-frequency signal reveals a spatially coherent decadal evolution. It is primarily a low-latitude phenomenon. Tropical SST anomalies peak in the central equatorial ocean with evidence of atmospheric teleconnections. These interdecadal and decadal signals join the ENSO and quasi-biennial signals in determining dominant patterns of Pacific Ocean natural climate variability. Relative phasing and location of the SST and SLP anomalies for the decadal, ENSO, and the quasi-biennial signals, are similar to one another but significantly different from that of the interdecadal signal.

Introduction

Global low-frequency climate variability has been identified (Mann and Park, 1996). In the Pacific Ocean and neighboring regions, patterns of low-frequency fluctuations within the climate and ecological systems have been referred to as the "Pacific (inter) Decadal Oscillation or PDO" (Mantua et al., 1997), the "Inter-decadal Pacific Oscillation or IPO (Power et al., 1999), the Pacific "Decadal and Interdecadal Climatic Event or DICE" (Nakamura and Yamagata, 1996) or as the "Bi-Decadal Oscillation or BDO" (Cook et al., 1997). Evidence also exists that low-frequency climate fluctuations modulate El Niño intensity (Torrence and Webster, 1999).

In this paper, joint relationships between SST and SLP anomalies for the Pacific Ocean are extracted based on spatial coherence at respective frequency bands, and show a significant distinction between decadal and interdecadal fluctuations. Relationships between these distinct low-frequency signals and the Pacific ENSO may assist in improving climate prediction (Gershunov and Barnett, 1998). Recent modeling results (e.g., Kleeman et al., 1999), should contribute to the evaluation of physical mechanisms associated with these climate fluctuations. By incorporating this new information into decision-making schemes (e.g., Meinke et al., 2000a), it is hoped global impacts of recurring drought/flood can be mitigated (Balmaseda et al., 1995).

Data and Results

A Multi-Taper-Method/Singular Value Decomposition (MTM/SVD) technique with three tapers (Mann and Park, 1999) is applied to 92 years (1900-1991) of SST and SLP gridded datasets (Kaplan et al., 1998). The three tapers allow for reasonable frequency resolution and provide sufficient degrees of freedom for a signal/noise composition. The joint local fractional variance (LFV) spectrum represents a fraction of variance in a particular narrow frequency band associated with slow temporal modulation. Stability of the analysis was tested by comparing results based upon the full period (1900-1991) and the 1950-1990 period. Impacts of systematic biases in data collection were tested by introducing artificial data gaps. A statistically significant separation of two low-frequency bands that represent independent information about spatially correlated oscillatory signals -- the interdecadal and the decadal/quasi-decadal signals -- is obtained. The spatial evolution of the signals is presented hereafter.

In Fig. 1, the LFV spectrum of the first joint SST-SLP singular values is displayed. The standardized anomalies are latitudinally weighted. The significance of peaks and frequency-bands in the LFV spectrum are determined through bootstrap time-resampling estimates (Efron, 1990) of the null
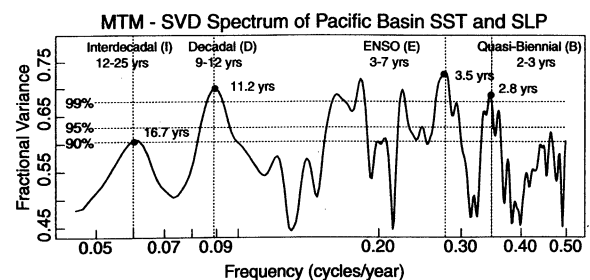
[1] Lamont Doherty Earth Observatory (LDEO)
[2] International Research Institute for Climate Prediction (IRI) of Columbia University, Palisades, NY
[3] Scripps Institution of Oceanography (SIO) of University of California San Diego, La Jolla, CA

Figure 1. LFV as a function of cycles-per-year (logarithmic scale starts at 0.04 cycle/year). Horizontal dashed lines represent the 99%, 95%, 90% averaged confidence levels. Vertical dashed lines represent the peak frequencies for the interdecadal (I), decadal (D), ENSO (E), and quasi-biennial (B) signals.
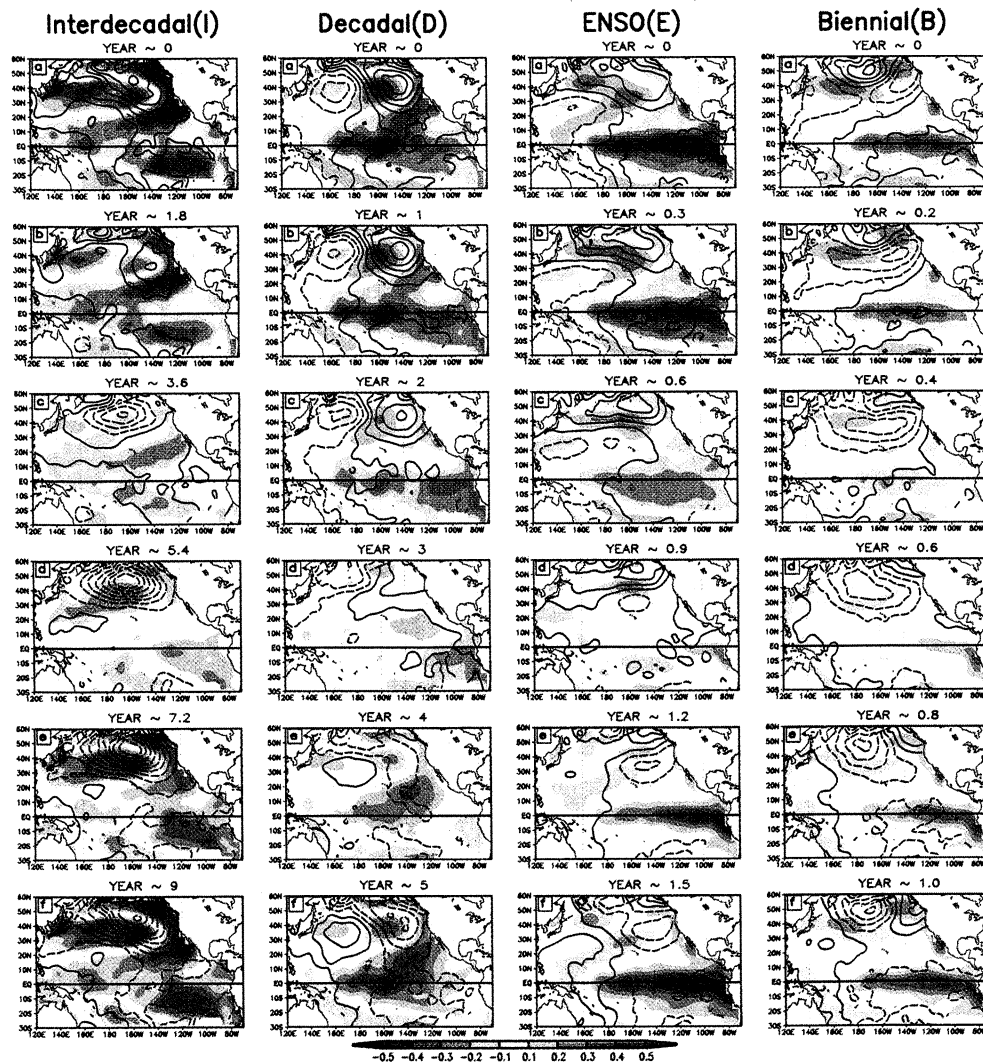
Figure 2. Spatial evolution of the interdecadal signal (left column), decadal signal (middle left column), ENSO signal (middle right column), and biennial signal (right column). The six frames in each column represent approximately half of each nominal cycle. Last frames represent phases with maximum positive SST anomalies in the tropics. SST anomalies are colored (in 1/10th of °C). SLP anomalies are contoured every 1/10th mb (solid lines for positive anomalies and dashed lines for negative anomalies) with a thick zero-contour line.

distribution of a spatio-temporal "colored noise". The potential bias from serial correlation was minimized by permuting 1000 times, at random and separately, for the 92-yr annual sequences for each of the 12 months of the year (Mann and Park, 1996). The interdecadal band peaks within the 16 to 17-year periods at the 90% confidence level (I in Figs. 1 and 2). The decadal band peaks within the 10.8 to 11.9-year periods at the 99% confidence level (D in Figs. 1 and 2). The ENSO band peaks at the 99% confidence level, within a range of 3 to 7-year periods (E in Figs. 1 and 2). Within this ENSO band, several peaks are less well separated from the noise background and are probably associated with other complex frequency-domain structures. The maximum LFV (~0.73) within the ENSO frequency-band peaks at a 3.5-year period. The evolution of this peak is characteristic of that of other ENSO peaks (above 99% confidence level) and so is reproduced in Figure 2. The quasi-biennial band (2 to 3-yr periods, B in Figs. 1 and 2) contributes significantly to the LFV spectrum. From Fig.1 the joint SST-SLP spatial patterns

and their evolution of the lead 16.7-year interdecadal (I), lead 11.2-year decadal (D), lead characteristic 3.5-year ENSO (E), and lead 2.8-year quasi-biennial (B) signals are reconstructed for one-half cycle. They are displayed in Figure 2 (left column for I, left middle column for D, right middle column for E, and right column for B, respectively), from maximum tropical cooling to maximum tropical warming.

For the interdecadal signal (Fig. 2, left column), SST and SLP anomalies evolution is very similar to that featured in Tourre at al. (1999). Midlatitude SLP anomalies are found to develop in the North Central Pacific around 45°N (Fig. 2, Ic). Significant midlatitude SST anomalies occur between 25°N-45°N and 170°E-160°W and amplify along the subarctic frontal zone (SAFZ) while SLP anomalies of the same polarity keep developing eastward and poleward (Fig.2, Id to If) indicating possible coupling and feedback mechanisms between the ocean and atmosphere there (Peng and Witaker, 1999). This is also the time when SST anomalies (with opposite polarity) develop rapidly along the North and South

American coastlines (Fig. 2, Ie and If). The offshore SST anomalies in the eastern ocean are probably maintained by anomalous oceanic vertical circulation associated with co-varying SST and SLP anomalies to the west, yielding along-shore wind anomalies. The portion of the SST anomaly pattern arising from possible advection of SST anomalies extends slowly equatorward following the Californian Current, the Humboldt Current, and the South Equatorial Current or SEC (Fig. 2, Id to If). The maximum anomalies in the North Pacific Ocean are not found south of 10°N, apparently due to the North Equatorial Counter Current. Conversely, the SST anomalies in the South Pacific Ocean penetrate all the way to the equator in the central and western Pacific Ocean. The hemispheric symmetry displayed in Figure 2 (left column) emphasizes the role of the general circulation in the tropical South Pacific Ocean advecting SST anomalies onto the equator via the SEC. During the tropical warm phase of the interdecadal signal, maximum SST anomalies in the eastern ocean are found away from the equator near 15°N and 15°S, and maximum SLP anomalies are found at 45°N possibly modulating the intensity of the Aleutian Low. In the western ocean SST anomalies occur on the equator between 160°E and the dateline, where maximum salinity and temperature gradients are usually found (Picaut et al., 1996). The tropical SLP fluctuations contribute to Southern Oscillation variability (Fig. 2, Ie and If). When, in the midlatitudes, SST anomalies of a given polarity decrease slowly along the SAFZ (Fig. 2, Ia to Ic) subduction from the outcrop region of the gyre occurs at 10-15 m/year while anomalies of upper-ocean heat content extend slowly southwestward within the subtropical gyre to reach the Philippines Seas 8-10 years later (Tourre et al., 1999).

For the decadal signal (Fig. 2, left middle column), SST anomalies are found to amplify from the northeast tropical Pacific into the central equatorial Pacific Ocean (Fig. 2, Dd to Df). Simultaneously SLP anomalies of opposite polarity amplify around 40°N, approximately within the same longitudinal band between 120°W and 160°W. SST anomalies of opposite polarity amplify in the midlatitudes around 40°N and between 140°W and the dateline, probably due to maximum wind action there and resultant mean Ekman transport in near surface mixed layer of the ocean (Auad et al., 1998b). Subsequent evolution of tropical SST anomalies, is reminiscent of slow ENSO boundary waves and Kelvin-Rossby wave dynamics (White et al., 1989) (Fig. 2, De and Df to Da and Db with opposite polarity). The development of midlatitude SLP anomalies in the northeast Pacific Ocean, suggests atmospheric teleconnections in response to SST-induced tropical convection, as on ENSO timescales (Graham, 1994). This mechanism is a good candidate for maintaining the year-to-year persistence of anomalous intensity of the Aleutian Low (Graham and White, 1988).

Discussion and Conclusion

Low-frequency climate variability in the Pacific Ocean consists at least of two spatially coherent signals in covarying SST and SLP anomalies: interdecadal and decadal signals, with distinct spatial evolutions that invoke different physical processes to maintain their amplitudes against dissipation. Additional evidence is presented here for the interdecadal signal to be maintained in the midlatitudes along the SAFZ through coupled ocean-atmosphere dynamics (see also Auad

et al., 1998b; White and Cayan, 1998; Barnett et al., 1999). The signal is then advected by the mean gyre circulation (White and Cayan, 1998), where it communicates back to the midlatitudes, possibly of both hemispheres via atmospheric teleconnections. As such, the interdecadal signal requires mean advection to provide for the necessary feedback and the characteristic timescale of the phenomenon. Decadal, ENSO, and quasi-biennial signals require Rossby wave physics to provide the feedback and the characteristic timescales. The low-frequency decadal oscillation or PDO as previously defined in the literature does not provide for the distinction between the interdecadal and decadal Pacific signals. Analysis based on spatial coherence of standing modes extracts two distinct spatial patterns of low-frequency variability in the North Pacific Basin (Barlow et al., 2000). The two spatial patterns are shown here to be two distinct "snapshots" in the evolution of the interdecadal signal (Fig. 2, d and f). Both spatial patterns are associated with stationary atmospheric wave activity projected across North America and significant variations in drought and wet spells there.

The distinct separation between the two low-frequency signals is further clarified through closer examination of the SLP evolution. With the interdecadal signal, the development of SLP anomaly in the North Pacific occurs before the development of local SST anomalies of the same polarity (Fig. 2, Ib and Ic). The North Pacific SLP anomalies switch polarity and are already large by the time the switch occurs in SST anomalies (Fig. 2, Id). With the decadal signal, the extratropical SLP and SST anomalies develop more or less together with same polarity.

Differences in the evolution of SST-SLP anomalies associated with I, D, E and B, are seen in the Tropics. The interdecadal tropical SST anomalies reach maximum values away from the equator near 15° latitudes (North and South), associated with the advection of anomalies by mean currents in both hemispheres. Tropical phasing of these interdecadal anomalies can modify the tropical ocean thermal and atmospheric pressure large scale patterns, contributing to the Southern Oscillation variability (Fig. 2, Ie and If) and possibly to the modulation of the intensity and evolution of El Niño (e.g., Kirtman and Schopf, 1998). We show here how the decadal signal evolves rapidly, from the central equatorial Pacific, into an ENSO-like pattern. This suggests that subtropical Rossby wave dynamics may be responsible for making the decadal signal evolve as an extended Pacific ENSO signal, providing the delayed-negative feedback mechanism that gives the decadal signal its characteristic time scale (e.g., Jacobs et al., 1994). We also suggest that the similarity in the evolution of D, E, and B is sufficient to hypothesize that the three signals share the same basic physics. The main similar feature is the development of large equatorial SST anomaly, with slightly lagged development of weaker extratropical anomaly of opposite sign around 40°N and from the central Pacific toward the northwest Pacific (decadal to quasi-biennial respectively). The development and phasing of SLP relative to SST anomalies in the midlatitudes is also quite similar among the three signals. In the tropics the three SLP signals contribute to Southern Oscillation variability with well-defined zero-line anomalies around the dateline (Fig. 2, Da, Ef and Bf). One of the difference among the three signals is that E and B originate in the southeast Pacific Ocean along the South American coastline, progressing westward along the equator. In contrast, D

evolves from the central equatorial Pacific Ocean and expands eastward along the equator. But some specific episodes have have evolved differently (Tourre and White, 1995).

Understanding the dynamics of low-frequency fluctuations may yield considerable predictive capabilities since low-frequency modes have been correlated with rainfall patterns in ENSO sensitive regions across the Indo-Pacific basin (Allan, 2000). Research involving climate and climate applications scientists in Australia and the UK (Meinke et al., 2000a) is investigating regional and near-global modulations of agricultural crops by distinct decadal-multidecadal signals in the climate system. The results presented here should yield improvement of Pacific ENSO prediction, intensity and evolution and help our community to move "beyond El Niño" (Navarra, 1999).

References

Allan, R. J., 2000: ENSO and climatic variability in the last 150 years. Chapter 1 in Diaz, H. F and Markgraf, V., (eds.), El Niño and the Southern Oscillation: Multiscale Variability, Global and Regional Impacts. Cambridge University Press, Cambridge, UK, 3-56.

Auad, G., A. J. Miller, and W. B.White, 1998b: Simulation of heat storages and associated heat budgets in the Pacific Ocean: Part 2. Interdecadal time scales. *J. Geophys. Res.*, 103, 27,621-27,625.

Balmaseda, M. A., M. K. Davey, and D. L. T. Anderson, 1995: Decadal and seasonal dependence of ENSO prediction skill. *J. Climate*, 8, 2705-2715.

Barlow, M., S. Nigam, and E. H. Herbery, 2001: ENSO, Pacific decadal variability and U.S. summertime precipitation, drought and riverflow. *J. Climate*, in press.

Cook, E. R., D. M. Meko, and C. W. Stockton, 1997: A new assessment of possible solar and lunar forcing of the bi-decadal drought rhythm in the Western united States. *J. Climate*, 10, 1343-1356.

Efron, B., 1990: The Jacknife, the bootstrap and other sampling plans. Memo. Society for Applied and Industrial Mathematics, 92 pp.

Gershunov, A., and T. P. Barnett, 1998: Interdecadal modulation of ENSO teleconnections. *Bull. Amer. Meteor. Soc.*, 79, 2715-2725.

Graham, N. E., and W. B. White, 1988: The El Niño cycle: a natural oscillator of the Pacific ocean-atmosphere system. *Science*, 240, 1293-1302.

Graham, N. E., 1994: Decadal-scale climate variability in the tropical and North Pacific during the 1970's and 1980's: Observations and model results. *Climate Dyn.*, 6, 135-152.

Jacobs, G. A., H. E. Hurlburt, J. C. Kindle, E. J. Metzger, J. L. Mitchell, W. J. Teague, and A. J. Wallcraft, 1994: Decade-scale trans-Pacific propagation and warming effects of an El Niño anomaly. *Nature*, 370, 360-363.

Kaplan, A., M. A. Cane, Y. Kushnir, A. C. Clement, M. B. Blumenthal, and B. Rajagopalan, 1998: Reduced space optimal interpolation of historical sea level pressure. *J. Geophys. Research*, 103, C9, 18567-18589.

Kirtman, B. P., and P. S. Schopf, 1998: Decadal variability in ENSO predictability and prediction. *J. Climate*, 11, 2804-2822.

Kleeman, R., J. P. McCreary Jr., and B. A. Klinger, 1999: A mechanism for generating ENSO decadal variability. *Geophys. Res. Lett.*, 26, 1743-1746.

Mann, M. E., and J. Park, 1996: Joint spatio-temporal modes of surface temperature and sea level pressure variability in the Northern Hemisphere during the last century. *J. Climate*, 9, 2137-2162.

Mann, M. E., and J. Park, 1999: Oscillatory Spatio-temporal Signal Detection in Climate Studies: A Multiple-Taper Spectral Domain Approach. *Advances in Geophysics*, 41, 1-131.

Mantua, N. J., S. R. Hare, Y. Zhang, J. M. Wallace, and R. C. Francis, 1997: A Pacific interdecadal oscillation with impacts on salmon production. *Bull. Am. Met. Society*, 78, 1069-1079.

Meinke, H., R. Stone, S. Power, S. Allan, R. Potgieter, and P. deVoil, 2000a: Analysis of decadal to multidecadal climate variability: Australian rainfall and impact on wheat crops. Proceedings of the 13th Australasian Forum on Climatology (ANZCF), 10-12 April 2000, Hobart, Australia, 33.

Nakamura, H., G. Lin, and T. Yamagata, 1997: Decadal Climate Variability in the North Pacific during the Recent Decades. *Bull. Am. Meteor. Soc.*, 10, 2215-2225.

Navarra, A. (ed.), 1999: Beyond El Niño: decadal and interdecadal climate variability. Springer-Verlag, Berlin, Germany. 374 pp.

Peng, S., and J. S. Whitaker, 1999: Mechanisms determining the atmospheric response to midlatitude SST anomalies. *J. Climate*, 12, 1393-1408.

Picaut, J., M. Ioualalen, C. Menkes, T. Delacroix, and M, J. McPhaden, 1996: Mechanism of the zonal displacement of the Pacific Warm Pool, implications for ENSO. Science, 274, 1486-1489.

Power, S., T. Casey, C. Folland, A. Colman, and V. Mehta, 1999: Inter-decadal modulation of the impact of ENSO on Australia. *Climate. Dyn.*, 15, 319-324.

Torrence, C., and P. J. Webster, 1999: Interdecadal changes in the ENSO-Monsoon system. *J. Climate*, 12, 2679-2690.

Tourre, Y. M., Y. Kushnir, and W. B. White, 1999: Evolution of interdecadal variability in sea level pressure, sea surface temperature, and upper ocean temperature over the Pacific Ocean. *J. Phys. Oceanogr.*, 9, 1528-1541.

Tourre, Y. M., and W. B. White, 1995: ENSO signals in global upper-ocean temperature. *J. Phys. Oceanogr.*, 25, 1317-1332.

White, W. B., Y. H. He, and S. E. Pazan, 1989: Off-equatorial westward propagating Rossby waves in the tropical pacific during the 1982-83 and 1986-87 ENSO events. *J. Phys. Oceanogr.*, 17, 264-280.

White, W. B., and D. R. Cayan, 1998: Quasi-periodicity and global symmetries in interdecadal upper ocean temperature variability. *J. Geophys. Res.*, 103, 21,335-21,354.

White, W. B., and D. R. Cayan, 2000: A global ENSO wave in surface temperature and pressure and its interdecadal modulation from 1900 to 1996. *J. Geophys. Res.*, (in press).

Zhang, J., W. Wallace, and D. S. Battisti, 1997: ENSO-like interdecadal variability: 1900-93. *J. Climate*, 10, 1004-1020.

Y. Kushnir, B. Rajagopalan, Y. M. Tourre, Lamont Doherty of Columbia University, Palisades, NY 10964, M. Barlow, International Research Institute, Palisades, NY 10964, W. B White, Scripps Institution of Oceanography of University of California San Diego, La Jolla, CA. 92037. (e-mail: tourre@ldeo.columbia.edu)